Ultrafast dynamics of finite Hubbard clusters: A stochastic mean-field approach

Denis Lacroix

Institut de Physique Nucléaire, IN2P3-CNRS, Université Paris-Sud, F-91406 Orsay Cedex, France

S. Hermanns, C. M. Hinz, and M. Bonitz

Christian-Albrechts-Universität zu Kiel, Institut für Theoretische Physik und Astrophysik, Leibnizstraße 15, 24098 Kiel, Germany

Finite lattice models are a prototype for interacting quantum systems and capture essential properties of condensed matter systems. With the dramatic progress in ultracold atoms in optical lattices, finite fermionic Hubbard systems have become directly accessible in experiments, including their ultrafast dynamics far from equilibrium. Here, we present a theoretical approach that is able to treat these dynamics in any dimension and fully includes inhomogeneity effects. The method consists in stochastic sampling of mean-field trajectories and is—for not too large two-body interaction strength—found to be much more accurate than time-dependent mean-field at the same order of numerical costs. Furthermore, it can well compete with recent nonequilibrium Green function approaches using second-order Born approximation, which are of substantially larger complexity. The performance of the stochastic mean-field approach is demonstrated for Hubbard clusters with up to 512 particles in one, two, and three dimensions.

I. INTRODUCTION

Experimental progress in the formation and manipulation of quantum optical lattices from one to three dimensions with the number of sites ranging from very few to thousands provide a perfect laboratory [1–4] for the study of nonequilibrium properties of mesoscopic bosonic and fermionic systems. Exciting recent observations include the expansions of fermions into an empty optical lattice [5], formation and expansion of fermionic pairs (doublons) in a lattice [6,7], e.g., the many-particle behavior following an interaction quench [8] or the transport behavior following a quench of the confinement potential [9]. This paves the way towards a fundamental understanding of interacting quantum systems, which is of prime importance for many areas of physics and chemistry, including ultracold atomic and molecular gases in traps and optical lattices, transport and coherence properties of macromolecules, superconductivity and magnetic properties of condensed matter systems on the nanoscale, thermodynamics of dense fermionic matter in compact stars, and so on.

The description of finite correlated quantum lattice systems out of equilibrium is very challenging. Exact solutions using direct configuration interaction (CI) methods are possible only for very small Hubbard clusters [10], and the use of quantum Monte Carlo methods [11] only slightly increases the accessible system size. These approaches are hampered by the exponential increase of the computational effort with the system size. For this reason, the interest in approximate nonequilibrium theories that are both reliable and efficient has recently increased substantially. The simplest approach to treat particle-particle interactions is via an effective average field, i.e., via mean-field theory [e.g., time-dependent Hartree-Fock (TDHF)]. However, with increasing quantum entanglement, this approximation quickly fails. Moreover, as we will show below (cf. Fig. 2), TDHF already fails for very small coupling strength (Hubbard-U).

To describe the systems and phenomena mentioned above, one has to resort to methods beyond mean-field, i.e., include correlation effects. In recent years, there has been remarkable progress in this direction, in particular, in the application to strongly out-of-equilibrium lattice systems. Among the successful approaches, we mention the time-dependent density matrix renormalization group method (TDDMRG) [8], e.g., time-dependent density functional theory (TDDFT) [12], e.g., nonequilibrium Green function (NEGF) [13–15], e.g., or time-dependent density matrix (TDDM) methods [13,16]. All these methods have various limitations, e.g., with respect to the correlation strengths (TDDFT, TDDM, NEGF) or the system dimensionality (TDDMRG). Recent benchmarks for the one-dimensional (1D) Fermi-Hubbard model indicated fundamental problems such as unstable behavior of TDDM [10] or unphysical damping in NEGF simulations [15] that could recently be overcome in part by applying the generalized Kadanoff-Baym ansatz (GKBA) [17–20]. At the same time, going beyond the mean-field level with these approaches is rather involved and very expensive in terms of computational resources.

We propose an alternative approach to correlated fermionic lattice systems where the simplicity of mean-field theory is combined with efficient stochastic methods that allow to incorporate correlation effects. This stochastic mean-field approach (SMF) has been recently developed and applied with success in nuclear physics [21–24]. We present tests against exact results for small lattice systems and demonstrate that SMF is accurate for weak to moderate coupling during the initial phase of relaxation. Moreover, applying it to large one-dimensional (1D), and to 3D systems—where no CI data are available—we demonstrate its impressive capabilities for extended systems.

Beyond mean-field transport theories

Most approaches going beyond the independent particle picture start from a generalized one-body equation of motion (EOM) where the effect of correlations associated to the

correlation matrix C_{12} is accounted for. For an ensemble of particles interacting through an (anti)symmetrized two-body interaction $\tilde{v}_{12}$, the exact evolution of the one-body density matrix reads ($[\cdot,\cdot\cdot]_-$ denotes the commutator and $\hbar \equiv 1$):

$$i\partial_t\rho = [h(\rho),\rho]_- + \tfrac{1}{2}\mathrm{Tr}_2[\tilde{v}_{12},C_{12}]_- \quad (1)$$

$$=: I^{\mathrm{MF}}[\rho] + I^{\mathrm{cor}}[C_{12}], \quad (2)$$

where $h(\rho) = T + V + \mathrm{Tr}_2(\tilde{v}_{12}\rho_2) =: T + V + U_{\mathrm{HF}}(\rho)$ is the mean-field Hamiltonian containing kinetic (T) and potential (V) energy and the potential U_{HF} that is induced by all particles. At the mean-field level, correlations are neglected leading to the TDHF theory. C_{12}, which is defined through the binary density operator via $\rho_{12} = \rho_1\rho_2(1 \pm P_{12}) + C_{12}$ (P_{12} is the pair permutation operator), is—in general—unknown. Theories that go beyond mean-field typically introduce approximations for the correlation matrix, $C_{12} = C_{12}[\rho]$ (e.g., TDDM), or the exchange-correlation potential V_{xc} (DFT). Similarly, within NEGF, corrections to TDHF are incorporated through the correlation self-energy $\Sigma[G]$. The standard strategy to improve mean-field is presented schematically in Fig. 1 (left part). Inclusion of correlation effects via the collision integral I^{cor}—even in a simplified version—in general leads to a much harder to solve problem compared to the original mean-field approximation. This becomes even more severe in nonequilibrium. Therefore, most standard approaches lead to a dramatic increase of the computational complexity of the problem and/or put significant restrictions on the system size or coupling strength that can be treated.
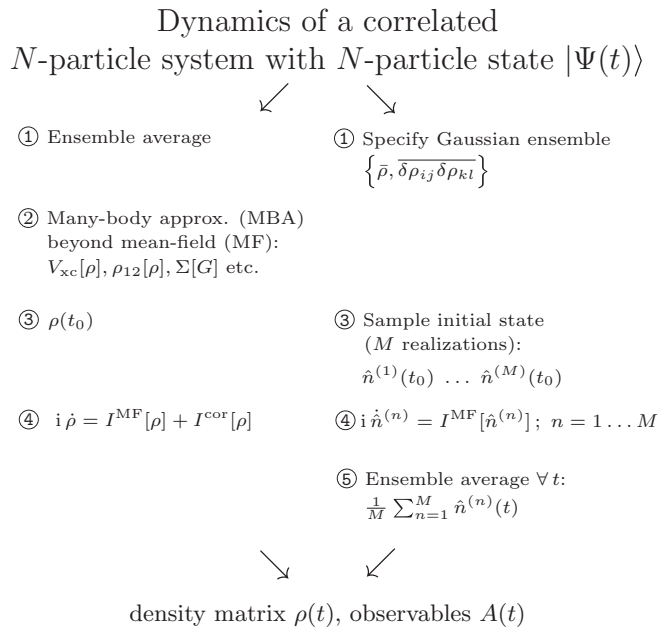
FIG. 1. Comparison of the strategy of typical many-body approaches (left) to the present stochastic mean-field method (right). Many-body approximations are specified, e.g., by the exchange-correlation potential V_{xc} (DFT), by the functional dependence of the two-body density matrix ρ_{12} on ρ or the form of the self-energy Σ (NEGF theory). In contrast, for the SMF, only TDHF trajectories are used and correlations are mimicked by a properly chosen ensemble.

II. STOCHASTIC MEAN-FIELD THEORY

The stochastic mean-field theory presents a fundamentally different strategy that aims at incorporating correlations (at least partially) while retaining the simplicity of a mean-field description.

A. General concept

We consider a stochastic scheme where an ensemble of single-particle density matrices $n^{(n)}(t)$ is used, where (n) labels a given realization (trajectory). In the following, we denote by $\bar{n}(t) = (1/M)\sum_M n^{(n)}(t)$ the average over the M trajectories and by $\delta n^{(n)}(t) = n^{(n)}(t) - \bar{n}(t)$ the individual fluctuations around this mean. Each density is assumed to evolve according to its own mean-field dynamic:

$$i\partial_t n^{(n)} = I^{\mathrm{MF}}[n^{(n)}] = [h(n^{(n)}),n^{(n)}]_-,$$
$$n^{(n)}(t_0) = n_0^{(n)}. \quad (3)$$

A straightforward derivation shows that the evolution of the average density is given by

$$i\partial_t\bar{n} = I^{\mathrm{MF}}[\bar{n}] + \overline{[\delta U_{\mathrm{HF}}(n^{(n)}),\delta n^{(n)}]_-}, \quad (4)$$

where $\delta U_{\mathrm{HF}}(n^{(n)})$ denotes fluctuations of the induced potential introduced by the density fluctuations. Additional discussions on Eq. (4) are provided in the Appendix A. Comparing this average evolution with Eq. (1), we see that evolving a statistical ensemble of densities can simulate the effect of correlations [25] provided that $\bar{n}(t) = \rho(t)$ and

$$\lim_{M\to\infty}\frac{1}{M}\sum_{n=1}^{M}\overline{[\delta U_{\mathrm{HF}}(n^{(n)}),\delta n^{(n)}]_-} = I^{\mathrm{cor}}[C_{12}]. \quad (5)$$

This correspondence is exact if condition (5) is fulfilled for all times, however, the correlation function $\overline{[\delta U_{\mathrm{HF}}(n^{(n)}),\delta n^{(n)}]_-}$ is of similar complexity as the pair correlation matrix C_{12}. To overcome this problem, the present stochastic mean-field approach proposes to map the time-dependent correlations onto fluctuations at the initial time t_0. Furthermore, the fluctuation spectrum is chosen such that it matches the quantum expectation value and fluctuations of the one-body density matrix (OBDM) of the initial state of the system (Gaussian approximation, details will be explained below for the Hubbard model). Then, each randomly chosen initial density is propagated in its own mean-field through Eq. (3) as is illustrated in the right part of Fig. 1. In this manner, we anticipate to achieve—at least for weak entanglement—correct correlated dynamics.

B. Physical interpretation of mean-field dynamics with fluctuating initial conditions

To get a better physical insight in the SMF approach, we give here an alternative view of the method based on a classical mapping of the initial quantum phase space. The heart of mean-field theory (such as Vlasov, Hartree, or Hartree-Fock) in the description of an interacting N-particle system is the reduction to an effective single-particle problem where interaction effects are condensed in an additional potential produced by all particles. All the information on the system

is contained in the expectation value of selected one-particle degrees of freedom (DOF, denoted by $\{\hat{A}_\lambda\}$) that evolve according to a set of coupled nonlinear equations:

$$\partial_t \langle \hat{A}_\alpha(t) \rangle = \mathcal{F}(\{\langle \hat{A}_\beta(t) \rangle\}). \qquad (6)$$

Two-body (and higher) expectation values $\langle \hat{A}_\alpha \hat{A}_\beta \rangle_{\text{MF}} = \langle \hat{A}_\alpha \rangle \langle \hat{A}_\beta \rangle + C_{\alpha\beta} \rightarrow \langle \hat{A}_\alpha \rangle \langle \hat{A}_\beta \rangle$ are factorized, thereby neglecting correlation contributions $C_{\alpha\beta}$ that are directly related to fluctuations around the mean values, $C_{\alpha\beta} = \langle (\hat{A}_\alpha - \langle \hat{A}_\alpha \rangle) (\hat{A}_\beta - \langle \hat{A}_\beta \rangle) \rangle$.

The lack of predictive power of mean-field generally stems from the inadequacy to describe the time evolution of quantum fluctuations and most importantly their effects on relevant DOF. For small mesoscopic systems, finite-size effects will further enhance the role of quantum zero point motion and proper treatment of correlations is required. Standard many-body approaches have developed elaborate many-body approximations (MBA) for $C_{\alpha\beta}$ in terms of single-particle expectation values $\langle \hat{A}_\alpha \rangle$ or, more generally, in terms of the single-particle density matrix ρ or Green's function G, which is sketched in the left part of Fig. 1. The practical limitations of these methods were mentioned in the introduction.

The direct correspondence between correlations and fluctuations gives access to a completely different approach to the treatment of correlations in many-body systems (right part of Fig. 1): Let us assume that, at initial time, a complex system is described by a density operator $\hat{D}(t_0)$. From this, the mean-values $\langle \hat{A}_\alpha(t_0) \rangle = \text{Tr}(\hat{A}_\alpha \hat{D}(t_0))$ and the quantum variance-covariance matrix, denoted by $\sigma_{\alpha\beta}^2$, of the DOF of interest can be computed. To mimic the initial state, a classical probabilistic picture is used where a set of classical variables $\{a_\alpha\}$ is introduced. These variables are associated to a certain probability $P(\{a_\alpha\})$ that is chosen to ensure that the mean value $\overline{a}_\alpha$ and the variance-covariance obtained by the classical average, $\Sigma_{\alpha\beta}$, both equal their quantum counterparts. Using standard Monte Carlo sampling, a set of initial values $\{a_\alpha^{(n)}(t_0)\}$ can be constructed, where (n) labels a given event. Each initial conditions is then evolved in time according to:

$$\partial_t a_\alpha^{(n)}(t) = \mathcal{F}\left(a_\alpha^{(n)}(t)\right). \qquad (7)$$

Such an approach is expected to be valid when the main source of effects beyond the independent particle picture stems from the initial correlations. Usually, such a quasiclassical approach is not expected to be valid for long times due to the correlations that are built up during the time evolution. These correlations are anticipated to increase as the interaction increases. In finite systems, finite-size effects enhance the effect of quantum fluctuations and SMF turns out to be rather effective [24]. In addition, SMF also allows to explore large amplitude dynamics in physical situations near a bifurcation point where spontaneous symmetry breaking can play a crucial role [22].

III. APPLICATION TO FERMIONIC HUBBARD CLUSTERS

A proof that the proposed SMF approach is able to describe correlated quantum lattice systems is challenging because mean-field per se is a poor approximation, even in the weak coupling limit (see top panel of Fig. 2 and discussion below).
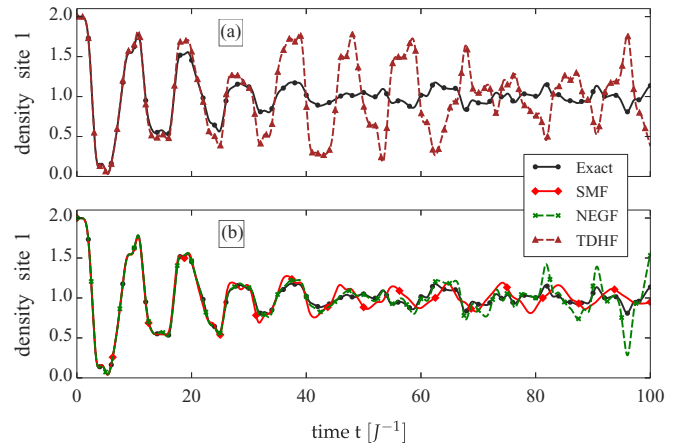
FIG. 2. (Color online) Time evolution of the leftmost site occupation $n_1(t)$ for $N_s = N = 8$ and $U/J = 0.1$. (a) CI (solid line) vs TDHF (dashes, triangles) and (b) CI vs NEGF (green, dashes) and SMF (red, diamonds).

It is the aim of this article to provide numerical evidence and to map out the parameter range where this approach works. In fact, we demonstrate that our SMF approach performs surprisingly well. Most importantly, since only standard mean-field evolution is needed, SMF does not face the catastrophic explosion of computational effort with system size as standard many-body theories.

A. Hubbard Hamiltonian

As an illustration of the capabilities of the SMF approach, a d-dimensional Hubbard nanocluster consisting of N_s doubly degenerate sites is considered. The time-independent part of the Hamiltonian in the canonical Hubbard basis reads:

$$H = -J \sum_{i,j}^{N_s} \sum_\sigma \delta_{\langle i,j \rangle} c_{i\sigma}^\dagger c_{j\sigma} + U \sum_i^{N_s} c_{i\uparrow}^\dagger c_{i\uparrow} c_{i\downarrow}^\dagger c_{i\downarrow}, \qquad (8)$$

where $\delta_{\langle i,j \rangle} = 1$ for nearest-neighbor sites and equals zero otherwise. Note that the dimensionality—and any boundary conditions—enter the Hamiltonian only via specifying which sites are nearest neighbors. This idealized Hamiltonian describes the interplay between strong localization and fast tunneling and was placed on the front of the stage by recent progress in cold atoms in optical lattices [28,29]. Mean-field dynamics provide a set of coupled equations for the OBDM $\rho_{ij,\sigma} = \langle c_{j\sigma}^\dagger c_{i\sigma} \rangle$, where σ denotes the spin orientation.

B. Implementation of the SMF approach

Within the SMF scheme, the initial OBDM is replaced by an ensemble of initial realizations, i.e., $\rho(t_0) \rightarrow \{n^{(n)}(t_0)\}$, each of which evolves according to Eq. (3) with the mean-field Hamiltonian

$$h(n^{(n)})_{ij,\sigma} = -J \delta_{\langle i,j \rangle} + U \delta_{ij} n_{ii,\bar{\sigma}}^{(n)}, \qquad (9)$$

where $\sigma = \uparrow (\downarrow)$ implies $\bar{\sigma} = \downarrow (\uparrow)$. The (random) initial configurations $\{n^{(n)}(t_0)\}$ in the Hubbard basis are determined by demanding that the matrix elements $\tilde{n}_{ij,\sigma}^{(n)}(t_0)$ of $n^{(n)}(t_0)$

satisfy

$$\overline{\tilde{n}_{ij,\sigma}^{(n)}(t_0)} = \delta_{ij}\tilde{n}_{i,\sigma}(t_0), \tag{10}$$

$$\overline{\delta\tilde{n}_{ij,\sigma}^{(n)}(t_0)\delta\tilde{n}_{kl,\sigma}^{(n)}(t_0)} = \frac{1}{2}\delta_{jk}\delta_{il}\tilde{n}_{j,\sigma}(t_0)[1 - \tilde{n}_{i,\sigma}(t_0)] \tag{11}$$

in the natural orbital basis of $\rho(t_0)$ with $\delta\tilde{n}_{ij,\sigma}^{(n)} = \tilde{n}_{ij,\sigma}^{(n)} - \overline{\tilde{n}_{ij,\sigma}^{(n)}}$, where $\tilde{n}_{i,\sigma}(t_0)$ denote the eigenvalues of $\rho(t_0)$. Here, only the first two moments of the density are constrained corresponding to a Gaussian ensemble (constraining higher moments as well may provide additional flexibility). At any time t, the expectation values of an arbitrary one-body observable can simply be computed as

$$\langle O(t) \rangle = \sum_{ij,\sigma} O_{ij,\sigma} \overline{n_{ij,\sigma}^{(n)}(t)}, \tag{12}$$

whereas the expectation value of a two-body observable T is given by

$$\langle T(t) \rangle = \sum_{ijkl,\sigma\tau} T_{ijkl,\sigma\tau} \left(\overline{n_{ij,\sigma}^{(n)}(t)} \; \overline{n_{kl,\tau}^{(n)}(t)} + \overline{\delta n_{ij,\sigma}^{(n)}(t)\delta n_{kl,\tau}^{(n)}(t)} \right). \tag{13}$$

It is worth mentioning that some flexibility exists in the mean-field evolution that is performed. For instance, in many situations, it might be advantageous to explicitly break a symmetry that is not broken in the exact evolution. This is for instance the case close to a bifurcation point or if a symmetry might spontaneously be broken at the mean-field level [22]. In the present Hubbard case, we might or not respect the spin symmetry in the dynamics. Spin symmetry is automatically included if the initial fluctuations of the density in the spin-up sector equal those in the spin-down sector. While the resulting densities look very similar in both cases, we observed that only by not imposing a spin symmetry (unrestricted case) we arrive at meaningful results for the different energy contributions to the total energy (see Sec. III D). For completeness, in Appendix B, we give the mean-field equation used in the unrestricted simulations as well as detail the choice of initial noise in the one-body density.

C. Application to a one-dimensional Hubbard lattice with half-filling

A first illustration is shown in Fig. 2 for a half-filled eight-site 1D chain without periodic boundary conditions at weak two-body interaction ($U/J = 0.1$) where we compare the exact solution and approximations. The initial state is chosen such that all eight electrons reside on the leftmost four sites. We see that even in the weak coupling regime, the mean-field result [TDHF, Fig. 2(a)] deviates very fast from the exact case and is, in particular, unable to describe the damping of the site occupation. In Fig. 2(b), we also show the NEGF-GKBA result obtained in second-order Born approximation [20], which performs much better (green, dashes). Finally, the SMF result obtained by using 10^4 fluctuating initial conditions is shown (red, diamonds). Obviously, SMF provides a dramatic improvement over TDHF, properly describes the short-time damping but also reasonably well describes the long-time dynamics until about $t = 75[J^{-1}]$. Note that, the considered
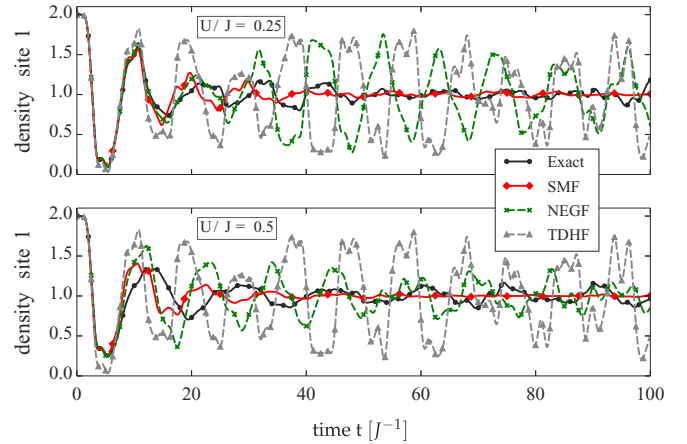
FIG. 3. (Color online) Time evolution of the leftmost site occupation $n_1(t)$ for $N_s = N = 8$, for $U/J = 0.25$ (top) and $U/J = 0.5$ (bottom). The exact solution (black solid line), NEGF (green, dashes) and SMF (red, diamonds) are shown. The SMF calculation are done using 10^4 initial conditions.

number of trajectories is already enough to have very small statistical error bars (not shown in Fig. 2). Increasing the number of trajectories would further reduce these error bars but does not change the average evolution in all figures shown below.

In particular, the revival observed at long times in the NEGF result ($t \sim 80, 90, 95[J^{-1}]$), is absent, in agreement with the exact case. For all particle numbers where CI data are available, in the weak coupling regime, we observe a similar accuracy of SMF, and, in most cases, the results are—apart from a different damping behavior—equally good compared to the NEGF ones.[1] When the interaction U/J increases, the overall behavior of the density is still correctly reproduced by SMF, in contrast to TDHF. At the same time, a quantitative agreement with CI is restricted to shorter times, cf. Fig. 3, comparable to the accuracy time observed in NEGF. Interestingly, in both NEGF and SMF, the validity range seems to be bounded by the correlation time of the system [20], $t \lesssim \tau_{cor} \sim 1/U$. In contrast to NEGF, for $U/J = 0.1$, the strength of the damping is well reproduced in SMF. When U/J is increased, it is observed that the damping is overestimated by SMF compared to the exact results.

D. Energy evolution

The SMF approach can give not only access to one-body observables but can also give interesting insight in quantities related to two-body effects. An illustration is given in Fig. 4 where the kinetic energy (E_{kin}), Hartree-Fock (E_{HF}) and correlation energies (E_{for}) are shown as a function of time in the SMF, NEGF, and exact case. In the latter two cases, these quantities are obtained by taking the quantum expectation

---

[1] For larger U, more accurate results can be achieved within the NEGF framework by choosing, e.g., the T-matrix approximation instead of second-order Born approximation [20].
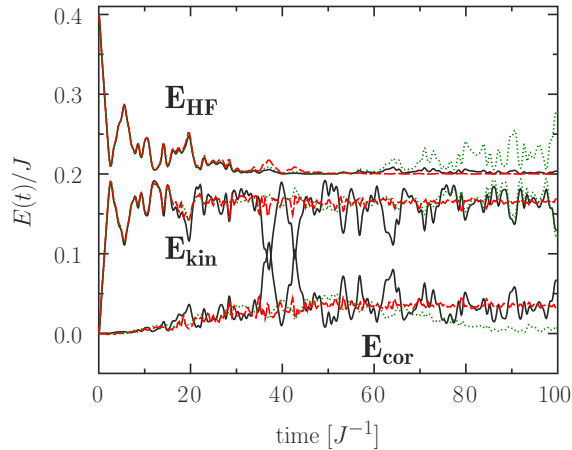
FIG. 4. (Color online) Evolution of the kinetic, HF and correlation energy obtained using the SMF approach (red dashed lines) for half-filling with $N_s = 4$ and $U/J = 0.1$. The three energies are compared to the exact case (black solid lines) and to the NEGF simulation of Ref. [20] (green dotted line). The SMF calculation are done using 10^4 initial conditions.

value:

$$E_{\mathrm{kin}} = -J \sum_{ij}^{N_s} \delta_{\langle i,j \rangle} (\langle c_{i\uparrow}^\dagger c_{j\uparrow} \rangle + \langle c_{i\downarrow}^\dagger c_{j\downarrow} \rangle),$$

$$E_{\mathrm{HF}} = +U \sum_{i}^{N_s} \langle c_{i\uparrow}^\dagger c_{i\uparrow} \rangle \langle c_{i\downarrow}^\dagger c_{i\downarrow} \rangle,$$

$$E_{\mathrm{cor}} = +\frac{U}{2} \sum_{i}^{N_s} \langle c_{i\uparrow}^\dagger c_{i\downarrow}^\dagger c_{i\downarrow} c_{i\uparrow} \rangle - E_{\mathrm{HF}}.$$

Analogous expression are used in the SMF theory except that quantum averages are replaced by classical ones, giving the definitions of the different energies:

$$E_{\mathrm{kin}}^{\mathrm{SMF}} = -J \sum_{ij}^{N_s} \delta_{\langle i,j \rangle} (\overline{n_{ij\uparrow}} + \overline{n_{ij\downarrow}})$$

$$E_{\mathrm{HF}}^{\mathrm{SMF}} = +U \sum_{i}^{N_s} \overline{n_{ii\uparrow}} \ \overline{n_{ii\downarrow}}, \quad E_{\mathrm{cor}}^{\mathrm{SMF}} = +U \sum_{i}^{N_s} \overline{\delta n_{ii\uparrow} \delta n_{ii\downarrow}}.$$

As discussed in Sec. II B, a classical mapping of the initial quantum phase space is made in the SMF approach. Accordingly, quantum fluctuations that are associated to correlation are obtained by performing classical averaging of the fluctuations. Here, this is illustrated in the estimate of the correlation energy. Figure 4 shows that, while not perfect, the SMF approach gives a very reasonable evolution of the different energy components and provides a good reproduction of the average trend. Both SMF and NEGF using the GKBA approach of Ref. [20] give reasonable results up to a time $t \sim 60 \, J^{-1}$, although they miss some of the oscillations of kinetic and correlation energy of the exact case. After this time (which corresponds to its validity range), the NEGF approach starts to deviate systematically from the exact evolution especially for the HF and correlation energy
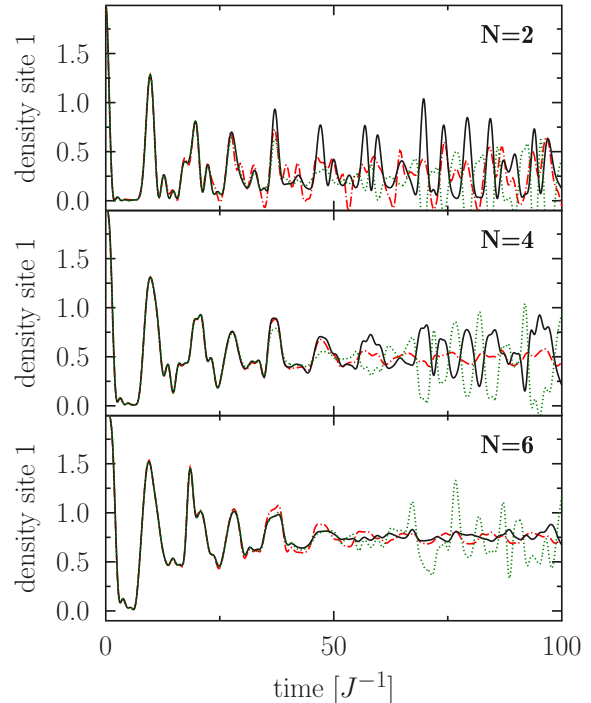
FIG. 5. (Color online) Leftmost occupation probabilities obtained with SMF (red dashed line) using 10^4 trajectories for the one-dimensional Hubbard systems with $U/J = 0.1$ and $N_s = 8$. From top to bottom, the case of $N = 2$, $N = 4$, and $N = 6$ particles positioned initially on the left side of the lattice are show. The SMF results are compared to the exact case (black solid line) and the NEGF approach of Ref. [20] (green dotted line).

whereas the one-body part (kinetic energy) remains very good (for a more detailed analysis of this approximation we refer to Ref. [20]). Most surprisingly, the SMF method continues to give a very reasonable average evolution of all quantities, including those related to correlations, even for longer time even though it does not capture the oscillations.

E. Application to the 1D Hubbard model away from half-filling

As a further illustration of the ability of SMF to grasp the dominant part of the correlations, we consider the same Hubbard setup with $N_s = 8$ sites but with less particles, $N = 2$, 4, or 6, initially occupying the left sites. Results of the dynamical evolution are shown in Fig. 5.

In all cases, the SMF approach gives almost perfect results for short times and starts to slightly deviate from the exact evolution for later times. The amplitude of oscillations around the average asymptotic limit is usually smaller than in the exact case but still remains reasonable. In particular, we do not see the revival of oscillations observed in the NEGF-GKBA approximation (see, e.g., the case $N = 6$).

In the extreme cases of two particles (two and four particles), we observe slightly negative occupation probabilities in the SMF (NEGF) simulations. However, these negative probabilities only occur at later times, i.e., beyond the validity range of the simulations, where we observe systematic deviations from the exact results in the $N = 6$ and $N = 8$ case. It is worth mentioning that such nonphysical behavior

has been already observed in theories based on the truncation of the one- and two-body density matrices evolution (see for instance Refs. [30] and [16]) when the allowed range of parameters is not explicitly built into the approximation. Therefore, it is not really surprising to observe them in the NEGF using the GKBA approximation since it is based on a similar hierarchy decoupling. In the case of two particles, we also observe the appearance of negative occupation numbers in SMF. While a dedicated study of this issue might be of interest in the near future, we anticipate that such nonphysical values stem from the Gaussian assumption made for sampling the initial density matrix components. In particular, unrestricted Gaussian sampling can lead to occupancies above 1 and/or below 0 for some events. A possible solution to this problem would be to assume a different initial sampling distribution that properly respects the density matrix boundary conditions. This would however significantly add complexity in the method, while we observe here that the bare Gaussian assumption already gives very good results in most cases.

F. Application to large systems

Since only mean-field evolutions are required, the numerical effort for SMF along each trajectory is the same as for TDHF. The main difference is that instead of a single trajectory, a set of mean-field trajectories is evolved in time. The number of trajectories is given by the number of initial conditions used to sample the initial quantum phase space. An additional simplification compared to other approaches like CI is that in SMF each trajectory is independent from all others. This makes the approach particularly suited for a massively parallel computation. As a consequence of these interesting features, the SMF can be applied to cases where other methods cannot be applied at all.

We illustrate this point in Fig. 6 where we apply SMF to long Hubbard chains of $N_s = 64$, 256 and 512 sites, respectively ($U/J = 0.1$) and where no exact solutions are available.
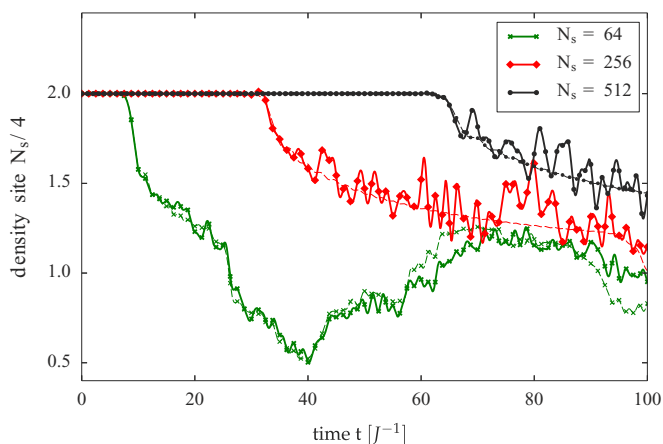
Starting from the same initial state as above (all N particles occupy the leftmost sites $1 \ldots N_s/2$) the occupation of the left sites first remains constant and then displays a rather complex evolution (Fig. 6 displays the initially occupied site $N_s/4$). The increase of the time before site depletion is due to the Pauli principle that prevents hopping until surrounding sites become at least partially empty. This time increases almost linearly with N_s indicating that, here, correlation effects are of minor importance. Also, the decrease of the population $n_{N_s/4}$ is strongly reduced with increasing N_s since—with the delay of depletion—particles initially located to the right have already undergone reflections at the right boundary and affect the originally occupied sites.

IV. APPLICATION TO TWO- AND THREE-DIMENSIONAL HUBBARD LATTICES

As a final illustration, we demonstrate that the SMF method can be directly applied to clusters of higher dimensions. In Fig. 7, we show, as an example, a cubic arrangement of 64 sites for half filling and weak coupling $U/J = 0.1$. As the initial configuration, we place all particles to the left half. Comparison of SMF to TDHF shows, as before, that mean-field is not adequate and strongly underestimates the damping, although the dominant frequency is correctly captured. We now try to understand the effect of the dimensionality. To this end, we compare to a 2D cluster of 16 sites (similar to a cut through the original cube) as well as to a linear chain of size $N_s = 4$ (see inset of Fig. 7). In all cases, the site occupations oscillate with almost the same main frequency. The most striking effect of dimensionality is that the damping of the oscillations grows when going from 3D to 1D.

This behavior is explained by the increasing number of particles, when going from 1D to 3D, undergoing the collective expansion. Dephasing effects that arise on the system boundary and lead to the damping are, thereby, systematically reduced. We mention that the expansion of one-dimensional fermionic

FIG. 6. (Color online) SMF result for large one-dimensional Hubbard systems with $U/J = 0.1$ and half filling for $N_s = 64$ (green), $N_s = 256$ (red), and $N_s = 512$ (black). The dynamics of the site occupation $n_{N_s/4}(t)$ are shown and compared to Hartree-Fock results (thin dashed lines). The SMF calculation are done using 10^4 initial conditions.
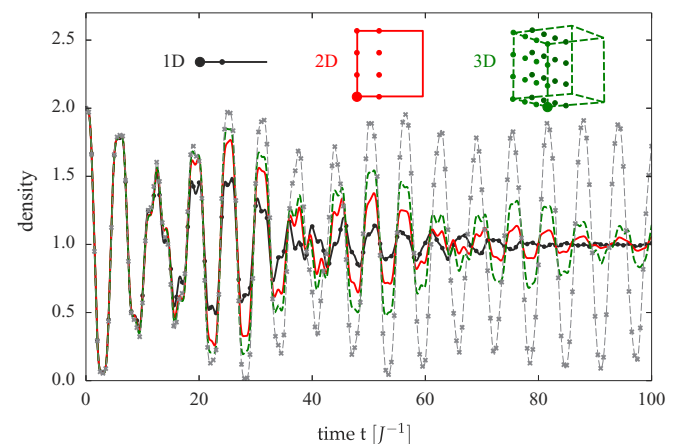
FIG. 7. (Color online) SMF result for a three-dimensional Hubbard cluster of size $4 \times 4 \times 4$, compared to a 2D (4×4) and 1D ($N_s = 4$) cluster (see inset for the initial state). The dynamics of the leftmost site (bold dot) occupation are shown and compared to the TDHF result (3D case, dashed line). The SMF calculation are done using 10^4 initial conditions.

systems into an empty optical lattice has been studied before for various setups, see, e.g., Ref. [5] and references therein. While our results are performed for a closed system, they indicate that details of the expansion with free boundaries might also vary with the system dimensionality.

V. CONCLUSION

In summary, we studied the ultrafast dynamics of finite spatially inhomogeneous fermionic Hubbard clusters with up to 512 sites in one, two, and three dimensions driven far from equilibrium. The results should be of interest for experiments and simulations of fermions in optical lattices, in particular for time-dependent expansion processes or quenches. Aside from these experimental situations our method should also allow to contribute to the understanding of fundamental theoretical questions such as the occurrence of thermalization [33] and its dependence on the systems size [34]. These studies were restricted to one-dimensional systems, and our approach brings the question of the dependence on the dimensionality within reach.

In this paper, we applied a stochastic mean-field approach where first a phase-space sampling of collective degrees of freedom is performed, followed by a set of simple time-dependent mean-field evolutions. We demonstrated that SMF significantly improves the mean-field dynamics—which rapidly fail already at weak coupling—by incorporating the effect of initial fluctuations of one-body degrees of freedom. Despite the fact that only a mean-field evolution is required, SMF can treat correlations and works very well, especially in the weak coupling regime. The main advantage is the very efficient inclusion of correlation effects via Monte Carlo sampling, which overcomes the unfavorable exponential scaling of wave function based approaches and allows to access large systems of arbitrary dimensionality. Here, the approach is implemented in its simplest form, i.e., starting from an uncorrelated state, where correlations are incorporated via Gaussian fluctuations of the initial site occupations. This, naturally, limits the method to the initial time stage, $t \lesssim \tau_{cor} \sim 1/U$, yet this regime is particularly interesting and difficult to treat since here correlations are being built up dynamically and Markovian approximations fail [31,32]. Extensions to longer times or/and stronger couplings seem to be straightforward, e.g., by inclusion of pairing correlations [23] or via time-dependent fluctuations. Finally, it is straightforward to extend the method to two-time fluctuations paving the way towards a stochastic approach to nonequilibrium Green function.

APPENDIX A: DETAILED DISCUSSION ON EQ. (4)

In the main text, we discuss two approaches to the time evolution of the one-body density matrix (see also Fig. 1): The first is for the density matrix ρ, Eq. (1). Here, ρ is associated to the reduced one-particle density operator that is derived from the full N-particle density operator of the system [13], $\hat{\rho} = N \mathrm{Tr}_{2...N} \hat{\rho}_{1...N}$. Equation (1) is standard text book material (see Eq. (3.20) of Ref. [13]). The second approach is to express the correlation terms via fluctuations. Here, we outline the main steps leading to Eq. (4).

We start with the one-particle density matrix operator $\hat{n}_{ij} \equiv \hat{a}_i^\dagger \hat{a}_j$ defined in terms of standard bosonic or fermionic creation and annihilation operators with respect to an arbitrary single-particle basis. Note that no ensemble averaging is applied yet.

The dynamics of $\hat{n}_{ij}$ is given by the Heisenberg equation

$$i\partial_t \hat{n}_{ij}(t) = -\hat{U}^\dagger(t,t_0)[\hat{H}(t),\hat{n}_{ij}]_- \hat{U}(t,t_0),$$
$$\hat{n}_{ij} := \hat{n}_{ij}(t_0), \tag{A1}$$

where $\hat{U}$ is the time evolution operator and $\hat{H}(t)$ the system Hamiltonian written in second quantization as

$$\hat{H} = \hat{T} + \hat{V} + \hat{W}, \tag{A2}$$

$$\hat{T} + \hat{V} = \sum_{ij} \hat{a}_i^\dagger (t_{ij} + v_{ij}(t)) \hat{a}_j, \tag{A3}$$

$$\hat{W} = \frac{1}{2} \sum_{ijkl} \hat{a}_i^\dagger \hat{a}_j^\dagger w_{ijkl} \, \hat{a}_l \hat{a}_k. \tag{A4}$$

Using these expressions and the (anti)commutation relations of the operators $\hat{a}_i^\dagger$ and $\hat{a}_j$, the commutator in (A1) is straightforwardly evaluated, with the result

$$i\partial_t \hat{\mathbf{n}}(t) = [\hat{\mathbf{n}}(t), \{\mathbf{t}^* + \mathbf{v}_H^*(t) + \hat{\mathbf{U}}_H^\pm(t)\}]_-. \tag{A5}$$

Here, we introduced bold notation for matrices of one-body operators, $\hat{\mathbf{n}} \equiv \hat{n}_{ij}$, and the subscript H designates a Heisenberg operator, i.e., $\hat{A}_H \equiv \hat{U}^\dagger(t,t_0) \hat{A} \, \hat{U}(t,t_0)$. Furthermore, the (antisymmetrized) induced potential appearing in (A5) is given by

$$\hat{U}_{kj}^\pm = \sum_{ln} \frac{w_{jnkl} \pm w_{jnlk}}{2} \{\hat{n}_{nl} \mp \hat{\delta}_{ln}\}. \tag{A6}$$

The final step is to perform an ensemble average of Eq. (A5), where we denote the average of an operator by $\langle \hat{A} \rangle \equiv A$ and express the two-operator average via the fluctuations $\langle \hat{A}\hat{B} \rangle = AB + \langle \delta\hat{A}\delta\hat{B} \rangle$, where $\delta\hat{A} = \hat{A} - A$. With these definitions, the ensemble average of Eq. (A5) is given by

$$i\partial_t \mathbf{n}(t) - [\mathbf{n}(t), \mathbf{t}^* + \mathbf{v}_H^*(t) + \mathbf{U}_H^\pm(t)]_-$$
$$= \langle [\delta\hat{\mathbf{n}}(t), \delta\hat{\mathbf{U}}_H^\pm(t)]_- \rangle \equiv \mathbf{I}^{cor}(t). \tag{A7}$$

The commutator on the left describes the mean-field dynamics (denoted I^{MF} in the main text), the term on the right is related to all contributions beyond mean field, i.e., to correlations.

Equation (A7) corresponds to Eq. (4) in the main text, where the short operator notation U_{HF} is being used for the Heisenberg matrix $\mathbf{U}_H^\pm$, and ρ is being used for the Heisenberg matrix $\mathbf{n}$. While Eq. (A7) is an equation for ensemble averaged quantities (corresponding to the left part of Fig. 1), Eq. (4) replaces the ensemble average by a classical average $\bar{n}$ over random realizations $n^{(n)}$, as is illustrated by the right part of Fig. 1.

APPENDIX B: EQUATION OF MOTION FOR THE UNRESTRICTED DYNAMICS

First, we write the TDHF equation allowing for a possible spin symmetry break by introducing the density matrix components in both spin sectors. The up and down components

of the density matrix read

$$n_{ij\uparrow} = \langle c_{j\uparrow}^\dagger c_{i\uparrow} \rangle, \quad n_{ij\downarrow} = \langle c_{j\downarrow}^\dagger c_{i\downarrow} \rangle. \tag{B1}$$

Starting from the Hubbard Hamiltonian for $N_s = M$, the two coupled mean-field equations of motion in the unrestricted case are given by:

$$
\begin{aligned}
i\partial_t n_{ij\uparrow} = &-J\{n_{(i+1)j\uparrow}(1-\delta_{iM}) - n_{i(j-1)\uparrow}(1-\delta_{j1}) \\
&+ n_{(i-1)j\uparrow}(1-\delta_{i1}) - n_{i(j+1)\uparrow}(1-\delta_{jM})\} \\
&+ U(n_{ii\downarrow} - n_{jj\downarrow})n_{ij\uparrow},
\end{aligned}
$$

and

$$
\begin{aligned}
i\partial_t n_{ij\downarrow} = &-J\{n_{(i+1)j\downarrow}(1-\delta_{iM}) - n_{i(j-1)\downarrow}(1-\delta_{j1}) \\
&+ n_{(i-1)j\downarrow}(1-\delta_{i1}) - n_{i(j+1)\downarrow}(1-\delta_{jM})\} \\
&+ U(n_{ii\uparrow} - n_{jj\uparrow})n_{ij\downarrow}.
\end{aligned}
$$

It can be checked that the mean-field energy, given by

$$
\begin{aligned}
E_{\mathrm{MF}} = &-J \sum_{i,\sigma=\uparrow,\downarrow} [n_{(i+1)i\sigma}(1-\delta_{iM}) + n_{(i-1)i\sigma}(1-\delta_{i1})] \\
&+ U \sum_i n_{ii\uparrow}n_{ii\downarrow},
\end{aligned} \tag{B2}
$$

is a constant of motion. For the unrestricted dynamics, the SMF is implemented using the initial fluctuations:

$$
\begin{aligned}
\overline{\delta n_{ij\uparrow} \delta n_{kl\downarrow}} &= 0, \\
\overline{\delta n_{ij\uparrow} \delta n_{kl\uparrow}} &= \tfrac{1}{2}\delta_{il}\delta_{jk}[\tilde{n}_{i\uparrow}(1-\tilde{n}_{j\uparrow}) + \tilde{n}_{j\uparrow}(1-\tilde{n}_{i\uparrow})], \\
\overline{\delta n_{ij\downarrow} \delta n_{kl\downarrow}} &= \tfrac{1}{2}\delta_{il}\delta_{jk}[\tilde{n}_{i\downarrow}(1-\tilde{n}_{j\downarrow}) + \tilde{n}_{j\downarrow}(1-\tilde{n}_{i\downarrow})].
\end{aligned}
$$

These fluctuations are complemented by

$$\overline{n_{ij\uparrow}} = \delta_{ij}\tilde{n}_{i\uparrow}, \overline{n_{ij\downarrow}} = \delta_{ij}\tilde{n}_{i\downarrow}.$$

[1] I. Bloch, J. Dalibard, and W. Zwerger, Rev. Mod. Phys. **80**, 885 (2008).

[2] L. Hackermüller, J. P. Ronzheimer, S. Will, S. Braun, T. Best, I. Bloch, E. Demler, S. Mandt, D. Rasch, and A. Rosch, Nature Phys. **8**, 213 (2012).

[3] D. Stadler, S. Krinner, J. Meineke, J.-P. Brantut, and T. Esslinger, Nature (London) **491**, 736 (2012).

[4] N. Strohmaier, D. Greif, R. Jördens, L. Tarruell, H. Moritz, T. Esslinger, R. Sensarma, D. Pekker, E. Altman, and E. Demler, Phys. Rev. Lett. **104**, 080401 (2010).

[5] S. Langer, M. J. A. Schuetz, I. P. McCulloch, U. Schollwöck, and F. Heidrich-Meisner, Phys. Rev. A **85**, 043618 (2012).

[6] J. Kajala, F. Massel, and P. Törmä, Phys. Rev. Lett. **106**, 206401 (2011)

[7] S. Keßler, I. P. McCulloch, and F. Marquardt, New J. Phys. **15**, 053043 (2013).

[8] J.-S. Bernier, R. Citro, C. Kollath, and E. Orignac, Phys. Rev. Lett. **112**, 065301 (2014).

[9] U. Schneider, L. Hackermüller, J. P. Ronzheimer, S. Will, S. Braun, T. Best, I. Bloch, E. Demler, S. Mandt, D. Rasch, and A. Rosch, Nature Phys. **8**, 213 (2012).

[10] S. Akbar Jafari, Iranian J. Phys. Res. **8**, 113 (2008).

[11] W. M. C. Foulkes, L. Mitas, R. J. Needs, and G. Rajagopal, Rev. Mod. Phys. **73**, 33 (2001).

[12] J. I. Fuks, M. Farzanehpour, I. V. Tokatly, H. Appel, S. Kurth, and A. Rubio, Phys. Rev. A **88**, 062512 (2013).

[13] M. Bonitz, *Quantum Kinetic Theory* (Teubner, Stuttgart, 1998).

[14] N. E. Dahlen and R. van Leeuwen, Phys. Rev. Lett. **98**, 153004 (2007).

[15] M. Puig von Friesen, C. Verdozzi, and C.-O. Almbladh, Phys. Rev. Lett. **103**, 176404 (2009).

[16] A. Akbari, M. J. Hashemi, A. Rubio, R. M. Nieminen, and R. van Leeuwen, Phys. Rev. B **85**, 235121 (2012).

[17] P. Lipavský, V. Špička, and B. Velický, Phys. Rev. B **34**, 6933 (1986).

[18] M. Bonitz, S. Hermanns, and K. Balzer, Contrib. Plasma Phys. **53**, 778 (2013).

[19] S. Hermanns, K. Balzer, and M. Bonitz, J. Phys. Conf. Ser. **427**, 012008 (2013).

[20] S. Hermanns, N. Schlünzen, and M. Bonitz, preceding paper, Phys. Rev. B **90**, 125111 (2014).

[21] S. Ayik, Phys. Lett. B **658**, 174 (2008).

[22] D. Lacroix, S. Ayik, and B. Yilmaz, Phys. Rev. C **85**, 041602(R) (2012).

[23] D. Lacroix, D. Gambacurta, and S. Ayik, Phys. Rev. C **87**, 061302(R) (2013).

[24] D. Lacroix and S. Ayik, Eur. Phys. J. A **50**, 95 (2014).

[25] The close relation of fluctuations to correlations has frequently been used to derive approximations for the correlation functions, e.g., in quantum electrodynamics [26] or plasma physics [27]. However, there it has not been used as a direct numerical tool.

[26] J. Schwinger, PNAS **37**, 452 (1951).

[27] Yu. L. Klimontovich, *Kinetic Theory of Nonideal Gases and Nonideal Plasmas* (Pergamon Press, Oxford, 1982).

[28] D. Jaksch, C. Bruder, J. I. Cirac, C. W. Gardiner, and P. Zoller, Phys. Rev. Lett. **81**, 3108 (1998).

[29] M. Greiner, O. Mandel, T. Esslinger, T. W. Hänsch, and I. Bloch, Nature (London) **415**, 39 (2002).

[30] K.-J. Schmitt, P.-G. Reinhard, and C. Toepffer, Z. Phys. A **336**, 123 (1990).

[31] M. Bonitz and D. Kremp, Phys. Lett. A **212**, 83 (1996),

[32] M. Bonitz, D. Kremp, D. C. Scott, R. Binder, W. D. Kraeft, and H. S. Köhler, J. Phys: Condens. Matter **8**, 6057 (1996).

[33] M. Rigol, Phys. Rev. Lett. **112**, 170601 (2014).

[34] W. Beugeling, R. Moessner, and M. Haque, Phys. Rev. E **89**, 042112 (2014).